Amplitude-Independent Longitudinal Ultrasonic Attenuation in Superconducting Lead*

W. A. FATE,† R. W. SHAW,‡ AND G. L. SALINGER
Rensselaer Polytechnic Institute, Troy, New York

(Received 28 February 1968)

The amplitude-independent attenuation of longitudinal ultrasound propagating in the [001] crystallographic direction in single-crystal superconducting lead was investigated, using the pulse-echo method, at frequencies between 10 and 210 MHz. Work was limited to lightly cold-worked high-purity lead and well-annealed tin- and thallium-doped lead where the amplitude independence of the results was experimentally demonstrated. The electron mean free path was evaluated for the specimens used in the experiment, and numerical data on the superconducting-to-normal electronic-attenuation ratio for well-characterized specimens are given for reduced temperatures greater than 0.6 where the data retain sufficient accuracy to be useful. The attenuation ratio derived from the measurements generally depends both on the ultrasonic frequency and impurity concentration, in disagreement with the prediction of the BCS theory. No unique value of the superconducting energy gap can be derived from the data using that theory. The decrease in the attenuation ratio near the transition is too rapid to be consistent with the BCS prediction. For reduced temperatures less than about 0.5 (depending on frequency and impurity concentration), the experimentally determined attenuation ratio decreases less rapidly than the BCS prediction. In pure deformed lead to temperatures where the mean freepath is phonon-limited, the attenuation ratio is frequency-dependent and departs from BCS most strongly for the lowest ultrasonic frequencies. This result is to be compared with recent results reported by Deaton for pure, well-annealed lead, where departures from BCS were found to be most pronounced at the highest ultrasonic frequencies. When the electron mean free path was impurity-dominated, the attenuation ratio was found to be nearly frequency-independent in the frequency range studied, but is dependent on impurity concentration. The data agree most closely with the BCS prediction for high-impurity concentrations. The frequency dependence of the electronic attenuation in the normal and superconducting states is in qualitative agreement with calculations of the electronic thermal conductivity, which show that the phonon-limited electron mean free path in the superconducting state is less than the corresponding free path in the normal state. An attempt is made to interpret the data semiquantitatively using this idea, and numerical estimates of the superconducting-to-normal ratio of an effective (energy-independent) phonon-limited free path are given in the reduced temperature interval $0.6 \leq t \leq 1.00$. The mean-free-path analysis reproduces the main qualitative freatures exhibited by the data just below the transition, but fails to quantitatively explain some of the less prominent features of the data in this temperature range. For reduced temperatures less than about 0.5, the mean-free-path mechanism is incapable of explaining the behavior of the observed attenuation ratio. The results of the present experiment are briefly compared with results recently reported by others.

I. INTRODUCTION

RESULTS of measurements of the low-temperature, amplitude-independent ultrasonic attenuation in normal lead have been reported in a previous article.[1] The main conclusion reached there is that amplitude-independent normal-state data are generally in good agreement with the predictions of the free-electron model provided it is assumed that the dislocation contribution to the low-temperature acoustic attenuation is temperature- and field-independent and the same in the normal and superconducting states. This shows that an amplitude-independent, temperature-dependent dislocation attenuation mechanism of the type proposed by Mason[2] cannot provide an adequate explanation for the anomalous superconducting-to-normal electronic-attenuation ratio which has been reported for lead.[3–7] Thus, the anomalous experimental results appear to be associated either with the superconducting electronic properties of lead or with the amplitude-dependent acoustic absorption that exists in this element.[3–5] It often proves difficult to experimentally eliminate amplitude-dependent effects, and in previous investigations[3–6] no experimental proof of the amplitude independence of the results was given. In this paper we present ultrasonic attenuation data for superconducting lead in some of those cases where the amplitude independence of the results was experimentally demonstrated. The experimental methods, including the method used to infer the amplitude independence of the results, have been given in I. The specimens used for

* This work was supported by the National Science Foundation and the National Aeronautics and Space Administration and is based on a thesis submitted by W. A. F. in partial fulfillment of the requirements for the Ph.D. degree at Rensselaer Polytechnic Institute.

† Present address: Scientific Laboratory, Ford Motor Co., Dearborn, Mich.

‡ Present address: Central Research Department, Monsanto Co., St. Louis, Mo.

[1] W. A. Fate, preceding paper, Phys. Rev. **172**, 402 (1968). This paper will hereafter be cited as I.

[2] W. P. Mason, Phys. Rev. **143**, 229 (1966).

[3] R. E. Love and R. W. Shaw, Rev. Mod. Phys. **34**, 260 (1964).

[4] R. E. Love, R. W. Shaw, and W. A. Fate, Phys. Rev. **138**, A1453 (1965).

[5] B. R. Tittmann and H. E. Bömmel, Phys. Rev. **151**, 178 (1966); *ibid.* **151**, 189 (1966).

[6] B. C. Deaton, Phys. Rev. Letters **16**, 577 (1966); Phys. Rev. (to be published). We thank Dr. Deaton for a report of some of his results prior to publication.

[7] W. A. Fate and R. W. Shaw, Phys. Rev. Letters **19**, 230 (1967).

TABLE I. Specifications of lead specimens.

Specimen number	Doping	State of anneal	l_r (cm)[a]	M (deg$^{-4.02}$)[a]
Pb No. 12	None	Deformed 0.25%	1.17×10^{-2}	5.18×10^{-3}
Pb No. 18	0.100 at. % Sn	Well annealed	3.42×10^{-4}	1.47×10^{-4}
Pb No. 21	0.100 at.% Tl	Well annealed	1.18×10^{-4}	0.517×10^{-4}
Pb No. 24	0.025 at.%Tl	Well annealed	4.32×10^{-4}	1.89×10^{-4}

[a] See Eq. (1).

that work were also used to obtain the present data. Data showing amplitude independence are presented in Fig. 2 of I. In all cases longitudinal sound was propagated parallel to the [001] crystallographic direction.

Some properties of the specimens used for the measurements are given in Table I. In the normal state the electron mean free path l is given by the formula[1]

$$l=l_r(1+MT^{4.02})^{-1}, \quad (1)$$

where l_r is the impurity-limited mean free path, M is a constant, and T is absolute temperature. The values of l_r and M appropriate to the various specimens are given in Table I.

Longitudinal ultrasonic attenuation data in superconductors are usually analyzed with the aid of the formula

$$R\equiv\alpha_s/\alpha_n=2f(\beta\Delta), \quad (2)$$

where α_s is the electronic attenuation in the superconducting state, α_n is the zero-field electronic attenuation that would be present in the normal state if the specimen did not become superconducting, and $f(x)=[1+\exp(x)]^{-1}$. In (2), $\beta=(k_BT)^{-1}$ and $\Delta(T)$ is the temperature-dependent energy-gap parameter of the BCS[8] theory. Equation (2) was first derived by BCS[8] for a weak-coupling superconductor with infinite electron mean free path. Subsequently, Tsuneto[9] showed that it also applies to a weak-coupling superconductor with arbitrary impurity-limited mean free path. The validity of (2) has never been established for weak-coupling superconductors in the phonon-limited case.

Recently it has been shown by Ambegaokar[10] and by Woo[11] that (2) also holds for strong-coupling superconductors in the limit of infinite frequency provided that the mean free path is phonon-limited and that the gap parameter of the BCS theory is replaced by the gap edge of the strong-coupling superconductor. For the strong-coupling case when the mean free path is phonon-limited, (2) does not hold for all frequencies; for arbitrary frequency the mean free paths and energy gaps for all electron energies now enter into integrals in a complicated way. Limited numerical calculations, valid for low frequencies and for temperatures near the transition temperature, have been performed by Woo,[11] but to date no calculations exist that are valid for all frequencies and temperatures of experimental interest. For strong-coupling superconductors in the impurity-limited regime, it is claimed[10] that the "gap edge" generalization of (2) holds for all ultrasonic frequencies. Explicit calculations in support of this conjecture have yet to appear.

Experimentalists usually assume that (2) is valid for arbitrary (phonon-limited, impurity-limited, and mixed) electron mean free paths and extract $\Delta(T)$ from attenuation ratio data using (2). No unique value of $\Delta(T)$ can be obtained from our data using this method. Furthermore, the values of $\Delta(0)$ deduced from the data using this method deviate significantly from the results of other experimental methods for determining the gap,[12] and also lie well outside the theoretical limits of gap anisotropy for lead given by the calculations of Bennett.[13] For purposes of comparing the data with (2) we assume that $2\Delta(0)=4.30k_BT_c$, which is consistent with the value obtained from tunneling data by Giaever and Megerle,[14] and is the value generally trusted by theorists. In addition we will assume that the temperature dependence of $\Delta(T)/\Delta(0)$ given by the BCS theory and tabulated by Mühlschlegel[15] is valid.

II. RESULTS

A. Qualitative Behavior

Figure 1 illustrates the main qualitative features exhibited by the experimentally determined attenuation ratio. Near the transition temperature R falls more rapidly than is consistent with the BCS formula. At intremediate reduced temperatures the data approach the theoretical attenutation ratio, and at the lowest temperatures the experimental attenuation ratio exceeds the theoretical one. Both the rapidity of the drop near the transition and the temperature at which the data cross the theoretical curve depend on frequency and impurity concentration. The low-temperature behavior

[8] J. Bardeen, L. N. Cooper, and J. R. Schrieffer, Phys. Rev. **108**, 1175 (1957).
[9] T. Tsuneto, Phys. Rev. **121**, 402 (1961).
[10] V. Ambegaokar, Phys. Rev. Letters **16**, 1047 (1966).
[11] J. W. F. Woo, Phys. Rev. **155**, 429 (1967).
[12] For a survey see D. H. Douglass, Jr., and L. M. Falicov, in *Progress in Low-Temperature Physics* (North-Holland Publishing Co., Amsterdam, 1964), Vol. 4, pp. 161 and 177.
[13] A. J. Bennett, Phys. Rev. **140**, A1902 (1965).
[14] I. Giaever and K. Megerle, Phys. Rev. **122**, 1101 (1960).
[15] B. Mühlschlegel, Z. Physik **155**, 313 (1959).

depicted in Fig. 1 is common to all the data: The attenuation ratio tends to zero at low temperatures less rapidly than is consistent with BCS. The following systematic features are to be noted: (1) When the mean free path is phonon-limited, R is frequency-dependent and departs from BCS behavior most strongly at the lowest ultrasonic frequencies. (2) When the mean free path is impurity-limited, R is nearly frequency-independent. In this case R depends on the concentration and type of impurities. (3) The data agree most closely with the BCS prediction in the impurity-limited case.

We next consider the determination of energy gaps from the present data. Writing (2) in the form

$$\ln[(2/R)-1]=[\Delta(0)/k_BT_c][G(t)/t], \qquad (3)$$

where $t=T/T_c$ and $G(t)=\Delta(T)/\Delta(0)$ is the reduced gap, we see that a plot of the left-hand side of (3) using experimental attenuation ratio data versus the theoretically given quantity $G(t)/t$ determines $\Delta(0)$ in units of k_BT_c as the slope of a straight line passing through the origin. A plot of this type for the 90-MHz Pb No. 12 data is shown in Fig. 2. Since the resulting curve is not a straight line, the temperature dependence of R given by (2) is not satisfied for any value of $\Delta(0)$. Curves similar to that of Fig. 2 were obtained for the doped specimens. For the pure deformed specimen at frequencies lower than 90 MHz, the departures from BCS behavior are qualitatively similar to, though more pronounced than, the deviations depicted in Fig. 2.

The zero-temperature gap derived from the low-temperature data ($t<0.5$) using plots of the type shown in Fig. 2 is sensitive to small errors in the determination of the nonelectronic component of the attenuation. This component of the attenuation will hereafter be called the background attenuation. If one allows small variations in the magnitude of the background attenuation, then different zero-temperature gaps result from the above analysis. For example, the low-temperature data of Fig. 2 gives a *full zero-temperature gap* of $2\Delta(0)=1.06k_BT_c$. If the background attenuation is raised

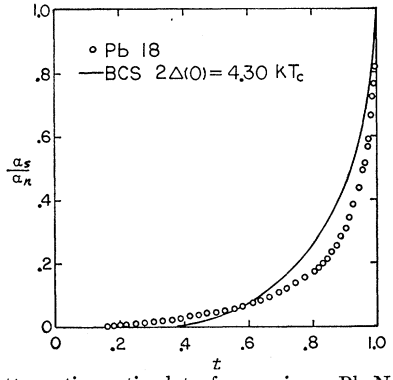

FIG. 1. Attenuation-ratio data for specimen Pb No. 18 compared with the BCS attenuation ratio. For this specimen the attenuation ratio is frequency-independent in the frequency range investigated and the data shown represent the average of data for five frequencies between 11.9 and 127 MHz.

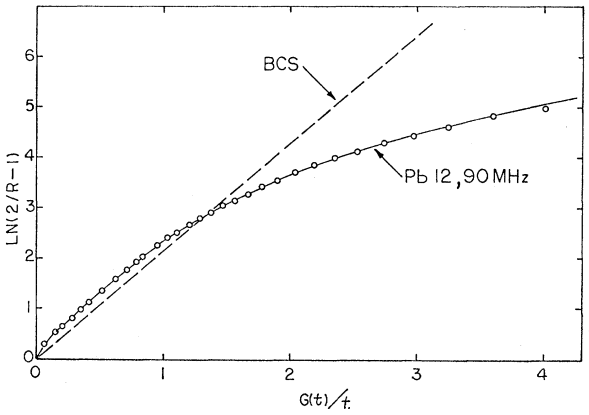

FIG. 2. Plot showing the difference in the temperature dependence of the BCS attenuation ratio and the measured attenuation ratio for Pb No. 12 at 90 MHz. The BCS curve is appropriate to a zero-temperature gap of $4.30k_BT_c$.

slightly and taken to be the value of the superconducting attenuation measured at 1.2°K, which corresponds to changing the background attenuation by 0.75% of the electronic attenuation at the transition, then the zero-temperature gap derived from the above analysis is $2\Delta(0)=1.86k_BT_c$. Since this is the largest value of the background attenuation that can legitimately be used, the latter gap value is the maximum zero-temperature gap consistent with both the low-temperature 90-MHz Pb No. 12 data and the BCS expression for the attenuation ratio. It was found that no reasonable choice of background results in reasonable zero-temperature gap values or in a curve linear over the entire temperature range of Fig. 2. To summarize, let us note the following: (1) The zero-temperature energy-gap values derived from the low-temperature data are sensitive to errors in the determination of the background attenuation. (2) The maximum zero-temperature gaps deduced from the data using the BCS formula are much smaller than the isotropic gap values determined by other experimental techniques,[12] and in pure lead depend on the frequency of measurement. The deviations from the generally accepted isotropic gap values are well outside the limits of gap anisotropy set by the semiempirical calculations of Bennett,[13] which, for lead, give $4.0k_BT_c\leq 2\Delta(0)\leq 4.7k_BT_c$. The low-temperature ultrasonic data typically give $2\Delta(0)=2k_BT_c$. (3) The large discrepancy between the zero-temperature energy gaps derived from the ultrasonic data and the gaps derived from other experiments, as well as the failure of (2) to fit the ultrasonic data for *any* choice of the zero-temperature gap and any reasonable background attenuation value shows that (2) does not furnish any criterion for the accurate determination of the background attenuation.

B. Data Analysis

The main factors limiting the accuracy of the attenuation ratio derived from the data are the uncertainty

in the value used for the background attenuation and possible errors in the superconducting and normal-state electronic attenuations. The uncertainty in the attenuation ratio, δR, was estimated from the equation

$$(\delta R)^2=\left(\frac{\delta\alpha_B}{\alpha_n}\right)^2\left(1-\frac{\alpha_s}{\alpha_n}\right)^2+\left(\frac{\alpha_s}{\alpha_n}\right)^2\left(\frac{\delta\alpha_n}{\alpha_n}\right)^2+\left(\frac{\delta\alpha_s}{\alpha_n}\right)^2, \quad (4)$$

where $\delta\alpha_B$, $\delta\alpha_n$, and $\delta\alpha_s$ are the uncertainties in the background attenuation, the normal-state electronic attenuation, and superconducting electronic attenuation, respectively. Equation (4) does not rigorously apply in the immediate neighborhood of the transition temperature, since there $\delta\alpha_n$ and $\delta\alpha_s$ are not independent. However, because of the rapid drop in α_s at the transition, the reduced temperature interval in which (4) fails to hold is very small. So (4) was used at all temperatures considered.

As in the analysis of the normal-state data given in I, the background attenuation is assumed to be temperature- and field-independent and the same in the normal and superconducting states. Since the low-temperature data deviate significantly from the temperature dependence predicted by (2), the often-used method of varying the background attenuation in an effort to find that background which, when subtracted from the data, give the best fit to the BCS temperature dependence of the attenuation ratio is not legitimate in the present case. Therefore, the background attenuation was determined by direct extrapolation of the measured superconducting attenuation to zero temperature. Generally the uncertainty in the background attenuation is between 1 and 2% of the electronic attenuation at the transition except for the pure deformed specimen at low frequencies where it is as much as 4% of the electronic attenuation at the transition. A small uncertainty in background leads to only a small uncertainty in the attenuation ratio near the transition, but is important for the analysis of the data at low reduced temperatures. In extreme cases the uncertainty in the attenuation ratio due to possible background error can amount to 100% at a reduced temperature of 0.50.

The accuracy of the determination of the zero-field normal-state attenuation differs for pure and doped specimens. For the doped specimens isothermal data of attenuation versus field strength show that the zero-field attenuation is approximated to within 2% by data taken in a transverse field of 940 Oe; for $T>5$°K the zero-field correction is negligible. No zero-field correction was applied to the 940-Oe data for the doped specimens.

The zero-field curve is more difficult to determine for the pure deformed specimen (Pb No. 12), since in this case a zero-field correction is required. The zero-field attenuation was determined at selected temperatures above 3.5°K by extrapolation of isothermal attenuation versus field strength data to zero field strength. In I the extrapolated zero-field data were compared with the Pippard[16] theory, and the rms deviation of the extrapolated data from that theory is within 5%. For the present analysis a smooth curve was drawn through the extrapolated points and α_n was determined at temperatures between the extrapolated data by interpolation. The interpolated data agreed with the Pippard calculation about as well as the extrapolated data did. Above 3.5°K the extrapolation errors in the normal-state curve, estimated to be between 1 and 5%, are largest near 3.5°K. For temperatures less than 3.5°K no zero-field extrapolations could be carried out because of magnetoacoustic effects. In this temperature range the mean-free-path estimates of I are most accurate and we used the ql estimates of I together with the value of the zero-field normal-state attenuation for infinite electron mean free path derived from the normal-state data, and calculated the low-temperature zero-field curve from the Pippard theory. At low temperatures, possible errors in background dominate the uncertainty in the attenuation ratio, hence the calculated zero-field curve was taken to be exact for $T<3.5$°K.

Besides errors in the normal-state attenuation due to errors in field extrapolations, the accuracy of the zero-field normal-state attenuation is influenced by possible errors in the attenuation measurements in nonzero field. Similar errors in attenuation measurement also affect the accuracy of the superconducting data. The accuracy of the attenuation measurements is determined by the precision of the attenuators used to calibrate the recordings of the amplitude of the gated echo, and this is determined by how well the attenuators are matched. Different matching networks were used for each ultrasonic frequency investigated, and errors in attenuator matching were estimated from the amount of scatter in isothermal attenuation versus input pulse amplitude data taken on amplitude-independent aluminum specimens as described in I. Effort was made to eliminate possible systematic errors that result when any particular pad of an attenuator gives an incorrect voltage reduction by calibrating the recordings in the usual way[4] at several different temperatures during each data run at a particular frequency. Since the signal levels at different temperatures differ because of the changing attenuation, this method allows the use of several different pad combinations to calibrate a given attenuation change. The results of the different calibrations usually agreed very well and were graphically averaged before data processing.

For the doped specimens the attenuation ratio derived from the data is different for different specimens, but for a given specimen is nearly frequency-independent over the frequency range investigated. For Pb No. 18 and Pb No. 21 no systematic change in the attenuation ratio with frequency was observed. For Pb No. 24 slight systematic frequency dependence of R was observed with R falling faster near the transition at the

[16] A. B. Pippard, Phil. Mag. **46**, 1104 (1955).

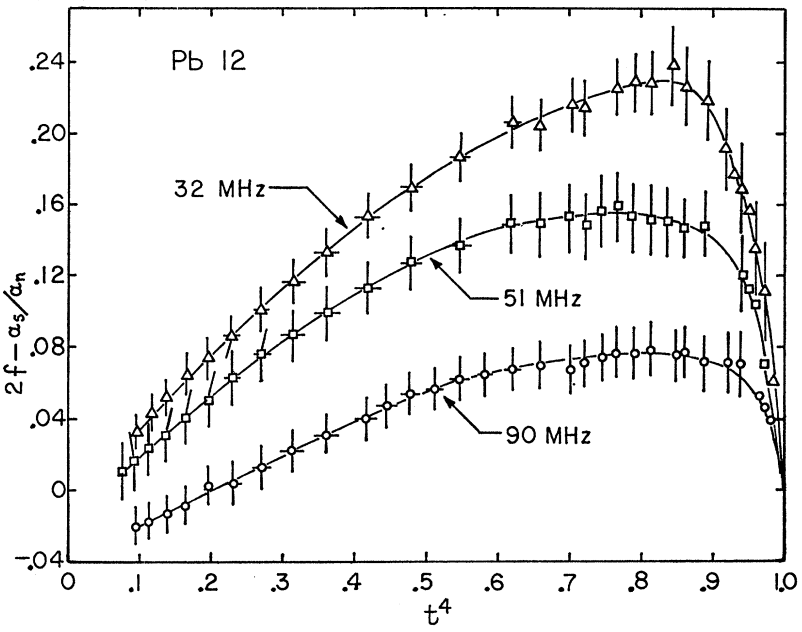

FIG. 3. Deviations from the BCS attenuation ratio for specimen Pb. No. 12 calculated under the assumption that $2\Delta(0)=4.30k_BT_c$. Uncertainty in this value as well as possible errors in frequency measurement have not been included in the uncertainty estimates. Some error bars have been omitted near $t=1$.

lowest frequencies, but the frequency dependence was within the limits set by (4). Therefore, for a given doped specimen, the attenuation-ratio data for the various frequencies were averaged. In these cases δR was calculated from (4), taking account of possible background errors and systematic errors in the normal-state curve below 5°K due to the (unmade) zero-field correction as described above, but the uncertainty in R due to possible matching errors, which should not be systematic from frequency to frequency, was estimated from the consistency of the data taken at the different frequencies.

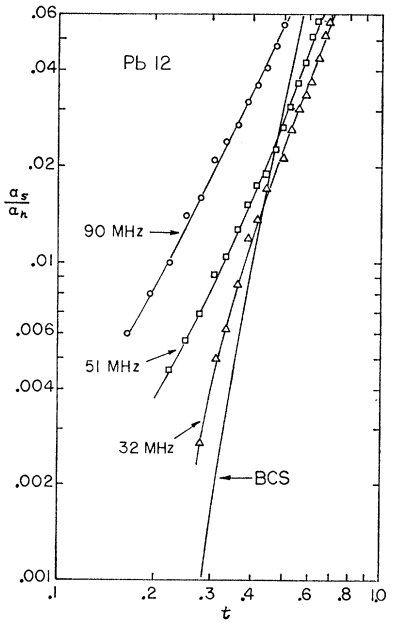

FIG. 4. Low-temperature attenuation-ratio data for specimen Pb No. 12. The BCS curve corresponds to a zero-temperature gap of $4.30k_BT_c$.

C. Data

Table II summarizes the attenuation ratio data for Pb No. 12 for reduced temperatures greater than approximately 0.6. Below this temperature the uncertainty in R is in the order of 100%. In I it was shown that the normal-state phonon-limited mean free path l_{ph} is given by $l_{ph}=2.27T^{-4.02}$ cm. This together with (1) and the data of Table I allows one to estimate the degree to which l is phonon-limited. For Pb No. 12 $l\geq 0.9l_{ph}$ for $t>0.87$ and $l\geq 0.8l_{ph}$ for $t>0.72$. Figure 3 shows the deviations of the measured attenuation ratio from the BCS attenuation ratio in the high-temperature range. The zero-temperature gap is taken to be $2\Delta(0)=4.30k_BT_c$; the uncertainty in this value, estimated to be $\pm 0.10k_BT_c$,[14] has not been included in the error estimates. Likewise, uncertainties in frequency measurement, estimated at $\pm 3\%$, have not been included in the uncertainties.

For low temperatures ($t\leq 0.50$) the data are very background sensitive, which precludes any precise analysis. However, it is to be observed that even if one takes the background attenuation to be the attenuation in the superconducting state at the lowest temperature reached ($t\simeq 0.18$), then the attenuation ratio tends to zero more slowly than is consistent with the BCS prediction. This effect, illustrated in Fig. 4, is common to all the data and does not vary significantly between pure and doped lead. We emphasize that the data of Fig. 4 are very background sensitive. At the lowest temperatures the attenuation ratio can be changed by several hundred percent by shifting the background slightly. However, the slow decrease in the attenuation

TABLE II. Attenuation ratio data for specimen Pb No. 12.

t[a]	R(12.8 MHz)[b]	R (32 MHz)[c]	R (51 MHz)[d]	R (90 MHz)[e]
0.996	0.794	0.821	0.836	0.837
0.993	0.750	0.729	0.772	0.792
0.990	0.721	0.678	0.710	0.756
0.988	0.696	0.640	0.683	0.733
0.985	0.674	0.601	0.650	0.699
0.971	0.554	0.473	0.538	0.616
0.964	0.509	0.426	0.507	0.575
0.957	0.459	0.389	0.472	0.548
0.950	0.419	0.367	0.444	0.515
0.943	0.387	0.341	0.417	0.493
0.936	0.353	0.320	0.386	0.468
0.922	0.300	0.286	0.353	0.429
0.916	0.278	0.267	0.328	0.413
0.901	0.239	0.241	0.298	0.378
0.888	0.209	0.209	0.264	0.347
0.860	0.162	0.171	0.220	0.295
0.832	0.129	0.141	0.183	0.256
0.805	0.105	0.113	0.153	0.223
0.777	0.088	0.094	0.128	0.197
0.749	0.079	0.078	0.106	0.171
0.722	0.066	0.065	0.089	0.153
0.693	0.057	0.053	0.077	0.136
0.666	0.052	0.043	0.067	0.114
0.638	0.044	0.034	0.057	0.107
0.610	0.037	0.029	0.051	0.095
0.583	0.034	0.024	0.043	0.084

[a] Reduced temperature uncertainty within ± 0.003 for $0.58 < t < 0.94$, within ± 0.001 for $0.94 < t < 1.00$.
[b] Approximate uncertainty in $R \pm 0.055$ for $1.00 > t \geq 0.86$, ± 0.030 for $0.86 > t > 0.58$.
[c] Approximate uncertainty in $R \pm 0.030$ for $1.00 > t \geq 0.96$, ± 0.015 for $0.96 > t > 0.58$.
[d] Approximate uncertainty in $R \pm 0.020$ for $1.00 > t \geq 0.93$, ± 0.015 for $0.93 > t > 0.58$.
[e] Approximate uncertainty in $R \pm 0.020$ for $1.00 > t \geq 0.95$, ± 0.010 for $0.95 > t > 0.58$.

ratio at low temperatures is insensitive to the exact value of the background used for the data analysis and is present in every case examined, in both pure and doped specimens. Love, Shaw, and Fate[4] erroneously concluded that this slow decrease is due to amplitude-dependent causes.

The 12.8-MHz data for Pb No. 12, not shown in Figs. 3 and 4, deviate from the systematic frequency dependence shown in Fig. 3. For reduced temperatures greater than 0.90 these data lie between the 32-MHz and the 51-MHz data of Fig. 3, while for $t < 0.90$ they are essentially identical to the 32-MHz data. Unfortunately there are large uncertainties associated with the 12.8-MHz data, which result because one must use low amplitudes (and hence low-order echos) to avoid amplitude-dependent effects. Since the electronic attenuation at low frequencies is small, and since high-order echos cannot be used to magnify the effect, the accuracy of the low-frequency data is poor. Figure 5 shows the 12.8-MHz data ($q = 366$ cm^{-1}) compared with the BCS result and the most (but not strictly) relevant strong-coupling calculation, that of Woo[11] valid in the phonon-limited case when $q = 320$ cm^{-1}. The latter calculation is confined to $0.95 \leq t \leq 1.00$.

Table III gives frequency-averaged attenuation ratio data for the doped specimens. A deviation plot for the thallium-doped specimens is shown in Fig. 6. Alloying not only quenches the frequency dependence of R, but also reduces the deviations of the measured R from the BCS attenuation ratio. This is in qualitative agreement with the claim[10] that the BCS formula holds in the impurity-limited case for strong-coupling superconductors. On the other hand, the low-temperature data for the doped specimens still show pronounced deviations of the type depicted in Fig. 4, while for the doped specimens l is impurity limited for $t \leq 0.50$.

D. Frequency Dependence

If the attenuation ratio were frequency-independent, in accord with the BCS prediction, the frequency dependence of α_s would be the same as the frequency dependence of α_n. When the attenuation ratio depends on frequency, as is the case for Pb No. 12, the electronic attenuation shows a different frequency dependence in the normal and superconducting states. In I it was shown that the ql and frequency dependence of α_n is in good agreement with the Pippard[16] free-electron attenuation theory. Since the background attenuation used for the analysis of the normal-state data was derived from the superconducting data as described above, an amplitude-independent dislocation mechanism, of the type proposed by Mason,[2] is probably not responsible for the anomalous attenuation ratio. The departures of the measured attenuation ratio from the BCS prediction thus appear to be electronic in origin and are associated with the superconducting state.

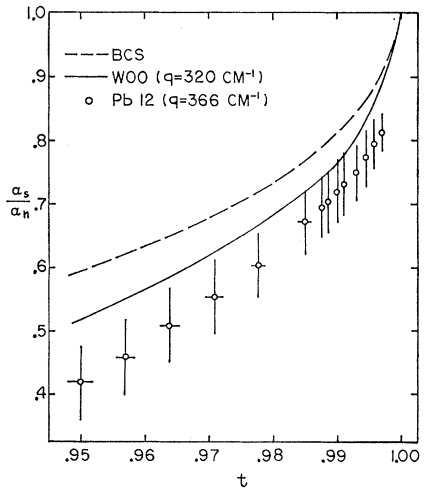

FIG. 5. 12.8-MHz data ($q = 366$ cm^{-1}) for Pb No. 12 compared with the BCS prediction and the calculation of Woo (Ref. 11), valid for $q = 320$ cm^{-1}.

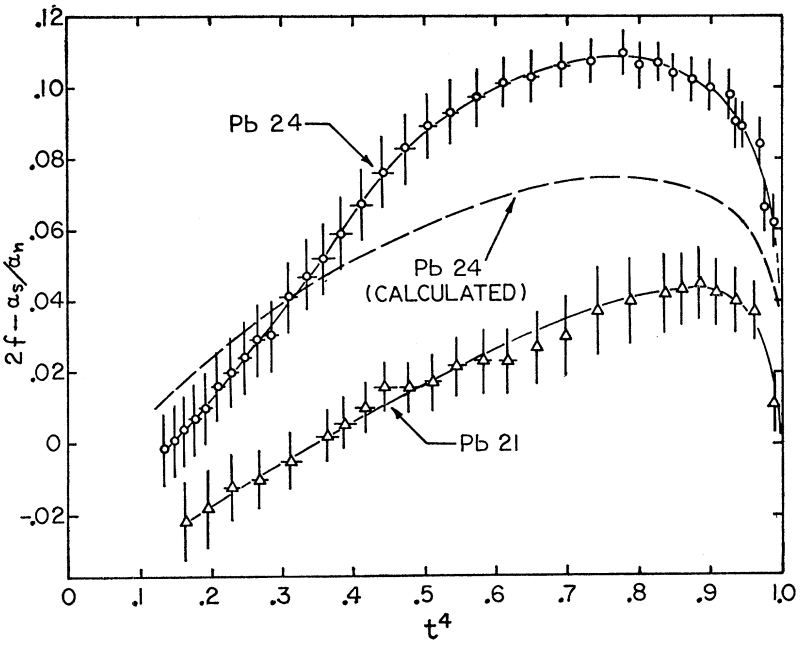

FIG. 6. Deviations from the BCS attenuation ratio for thallium-doped specimens. The impurity-limited mean free paths for Pb No. 21 and Pb No. 24 are 1.18×10^{-4} and 4.32×10^{-4} cm, respectively. The calculated curve is explained in Sec. II E.

TABLE III. Frequency-averaged attenuation-ratio data for doped specimens.

Pb No. 18		Pb No. 21		Pb No. 24	
t[a]	R[b]	t[a]	R[c]	t[d]	R[e]
0.996	0.818	0.997	0.889	0.997	0.838
0.990	0.723	0.990	0.775	0.989	0.717
0.985	0.665	0.983	0.716	0.983	0.668
0.975	0.589	0.976	0.671	0.974	0.602
0.971	0.564	0.970	0.636	0.967	0.565
0.963	0.516	0.963	0.605	0.960	0.531
0.957	0.490	0.956	0.576	0.953	0.500
0.943	0.436	0.942	0.525	0.946	0.474
0.929	0.386	0.928	0.483	0.925	0.403
0.915	0.345	0.914	0.447	0.912	0.367
0.902	0.310	0.900	0.416	0.898	0.335
0.888	0.282	0.886	0.388	0.884	0.305
0.873	0.253	0.873	0.361	0.870	0.281
0.860	0.235	0.859	0.334	0.856	0.258
0.844	0.213	0.845	0.314	0.843	0.238
0.832	0.199	0.831	0.292	0.829	0.221
0.817	0.185	0.817	0.269	0.815	0.206
0.805	0.172	0.803	0.253	0.801	0.193
0.776	0.152	0.776	0.223	0.773	0.170
0.749	0.134	0.748	0.197	0.746	0.149
0.720	0.118	0.720	0.174	0.718	0.133
0.694	0.104	0.693	0.152	0.691	0.118
0.638	0.082	0.637	0.120	0.649	0.098
0.612	0.073	0.609	0.105	0.622	0.086
0.582	0.065	0.582	0.095	0.594	0.077

[a] Reduced temperature uncertainty within ±0.003 for $0.58\leq t<0.94$, within ±0.001 for $0.94\leq t\leq1.00$.

[b] Average of data for five frequencies between 11.9 and 127 MHz. The uncertainty in R is ±0.010 for $0.90\leq t\leq1.00$ and ±0.012 for $0.58\leq t<0.90$.

[c] Average of data for three frequencies between 91.7 and 208 MHz. Uncertainty in R within ±0.012.

[d] Reduced temperature uncertainty within ±0.004 for $0.58\leq t<0.92$, within ±0.002 for $0.92\leq t\leq1.00$.

[e] Average of data for four frequencies between 32 and 205 MHz. Uncertainty in R within ±0.010.

According to the Pippard theory, the normal-state electronic attenuation α_n [denoted by $\alpha(0, ql)$ in I] is given by

$$\alpha_n=\alpha(0,\infty)F(ql), \tag{5}$$

where $\alpha(0,\infty)$ was evaluated in I:

$$\alpha(0,\infty)=0.18\nu \text{ dB/cm}, \tag{6}$$

ν being the ultrasonic frequency in MHz, and

$$F(x)=\frac{6}{x\pi}\left[\frac{1}{3}\frac{x^2\tan^{-1}(x)}{x-\tan^{-1}(x)}-1\right]. \tag{7}$$

For $x\leq\frac{1}{2}$, $F(x)=8x/5\pi$, so that from (5)–(7), α_n is proportional to ν^2 in the low-ql limit.

Figure 7 shows the frequency dependence of the superconducting and normal-state electronic attenuations for Pb No. 12 and Pb No. 18 at 6.5°K. In Fig. 7(a) the solid line labeled "Pippard" is calculated from (5)–(7) using l as given by (1). The normal-state data are in reasonable agreement with the frequency dependence predicted by the Pippard calculation, but the superconducting data show the expected frequency dependence only in the low-frequency limit. Over the frequency range investigated the superconducting data display an approximate ν^2 dependence, shown by the solid line labeled "square," which has been fit to the data by the method of least squares. The dashed line labeled "square" shows what is to be expected if the normal-state data obey a frequency square law and coincides with the Pippard curve at low frequencies where such a dependence is expected on theoretical grounds. At 90 MHz, the highest frequency investigated for this specimen, this square law gives a normal-state attenua-

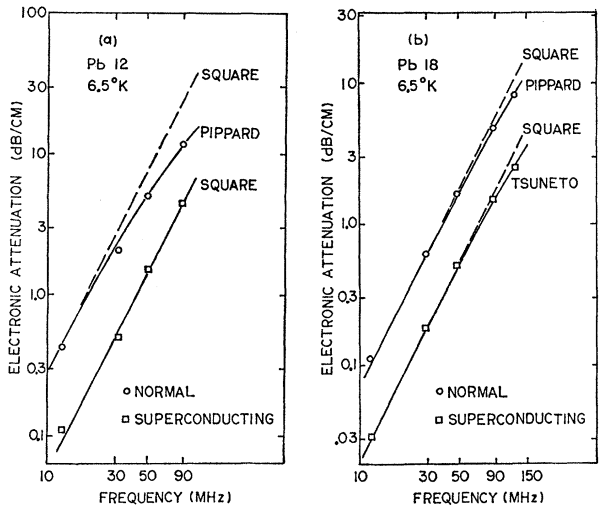

FIG. 7. Frequency dependence of the normal and superconducting electronic attenuation at 6.5°K. (a) Pb No. 12 and (b) Pb No. 18. See text for meaning of symbols.

tion in excess of twice the observed value. The frequency dependence of the superconducting data depicted in Fig. 7(a) was observed for Pb No. 12 at all temperatures between the transition and 5.5°K.

Figure 7(b) shows the analogous plot for the Pb No. 18 data. Here the curve label "Pippard" was calculated in the same way as before. The curve labeled "Tsuneto" shows the values calculated from the Pippard theory multiplied by 0.310, the mean attenuation ratio for Pb No. 18 at 6.5°K, and shows what is expected on the basis of (2). The ν^2 dependence determined by the low-frequency behavior is shown by the dashed lines labeled "square." At 127 MHz, the highest frequency investigated for Pb No. 18, the square law predicts an attenuation that exceeds the one predicted by the Pippard formula by 25%. Although the attenuation ratio is not in agreement with the BCS prediction, the frequency dependence of the superconducting and normal-state attenuations is in essential agreement with the theory and the attenuation ratio is frequency-independent.

For Pb No. 12 at 6.5°K, $l/l_{\rm ph}=0.905$, while at the same temperature for Pb No. 18, $l/l_{\rm ph}=0.220$. In the former case l is approximately phonon-limited and in the latter case l is dominated by impurity scattering. As has been briefly discussed elsewhere,[7] the difference in the frequency dependence of the electronic attenuation in these two cases suggests that the electron mean free path changes in the superconducting transition when l is phonon-limited. Indeed, such a change in the free path has already proved crucial for a semiquantitative understanding of the electronic thermal conductivity of superconducting lead in the phonon-limited case.[17] The present data suggest that in the phonon-limited case, the mean free path in the superconducting state is less than in the normal state. This is in qualitative agreement with the calculations of Ambegaokar and Woo,[17] which show that the superconducting-to-normal ratio of the energy-dependent, phonon-limited free path is less than unity. On the other hand, it is expected that the impurity-limited mean free path is the same in the two states.[10,11]

Let us now consider the consequences of the hypothesis that the phonon-limited electron mean free path alone changes in the superconducting transition and is less in the superconducting state than in the normal state. First, it is clear that when l is phonon-limited ($l/l_{\rm ph}\simeq 1$), the superconducting and normal-state attenuations will exhibit different frequency dependences since ql will be different for the two states. There should be no such difference, however, when l is impurity-limited ($l/l_{\rm ph}\ll 1$). If now one assumes that the weak-coupling theory gives qualitatively correct results, then from (2) and (5)

$$\alpha_s=\alpha(0,\infty)F(ql_s)2f(\beta\Delta), \qquad (8)$$

where l_s is an effective, energy-independent electron mean free path in the superconducting state. It follows that for the phonon-limited case, α_s can show a frequency square dependence at temperatures where α_n departs from such a dependence. It also follows from (8) that in the impurity-limited case such an effect should be absent.

Since the phonon-limited electron mean free path is known to be dependent on electron energy,[17] the above treatment is not rigorously correct. Even if $l_{\rm ph}$ was the same in the normal and superconducting states, the energy dependence of $l_{\rm ph}$ would cause an apparent lowering of the mean free path in the transition. Ambegaokar and Woo (see Fig. 6 of Ref. 17) have shown that in the normal-state $l_{\rm ph}$ is largest at the Fermi level and decreases as one goes away from the Fermi energy. Near the transition temperature as the gap opens up it is the low-energy excitations with long mean free paths that are condensed first because $l_{\rm ph}$ has its maximum at the Fermi level. The highly damped excitations are left above the gap, and these are the electrons that are responsible for the attenuation of the acoustic wave. Thus, even in the absence of a difference between the superconducting- and normal-state phonon-limited free paths, the average free path of the electrons that cause the attenuation in the superconducting state is lower than the average free path of the electrons that attenuate in the normal state. At a given energy the superconducting and normal phonon-limited free paths differ, so that in practice one observes a superposition of the two effects. Since these cannot be resolved experimentally, the l_s in (8) must be defined operationally to include not only the actual lowering of $l_{\rm ph}$, but also the additional apparent lowering of $l_{\rm ph}$ caused by

[17] V. Ambegaokar and J. Woo, Phys. Rev. **139**, A1818 (1965).

the condensation of the long free path electrons. From (5) and (8)

$$\alpha_s/\alpha_n=[F(ql_s)/F(ql)][2f(\beta\Delta)], \qquad (9)$$

which can be compared with data only if l_s is known.

E. Mean-Free-Path Analysis

One can extract l_s from attenuation ratio data, under the assumption that (9) holds, by using the normal-state mean free path given by (1). With the further assumption that the phonon-limited mean free path alone changes in the transition, it is possible to compute the superconducting-to-normal ratio of the phonon-limited free path, $l_{ph\,s}/l_{ph}$. This analysis was carried out using the attenuation ratio data for Pb No. 12 taken at 51 MHz. Numerical estimates of $l_{ph\,s}/l_{ph}$ so derived are given in Table IV, and the results are shown in Fig. 8. Figure 8 also shows $l_{ph\,s}/l_{ph}$ appropriate to an electron energy of 0.6 meV calculated by Ambegaokar and Woo.[17] Some difference between the two results may be expected since the quantity derived from our data is the ratio of the energy-average mean free path in the superconducting and normal states. While the free-path ratio calculated by Ambegaokar and Woo appears to have a finite slope at $t=1$ (see also Fig. 7 of Ref. 17), the effective free-path ratio deduced from the present analysis has a very large, if not infinite ,slope at the transition. Thus it is probable that the effective superconducting mean free path derived from our data includes effects other than a strict temperature dependence of the mean-free-path ratio.

TABLE IV. Superconducting-to-normal ratio of the averaged phonon-limited electron mean free path.

t	$l_{ph\,s}/l_{ph}$	t	$l_{ph\,s}/l_{ph}$
0.99	0.76	0.84	0.38
0.98	0.72	0.80	0.32
0.96	0.64	0.76	0.28
0.94	0.57	0.72	0.23
0.92	0.54	0.68	0.20
0.90	0.49	0.64	0.18
0.88	0.45	0.60	0.17

Using the superconducting mean free path just derived, we compare the deviations from the BCS prediction calculated from (9) with the experimentally observed deviations for Pb No. 12 at frequencies other than 51 MHz in Figs. 9 and 10.

In a similar way the curve labeled "Pb 24 calculated" in Fig. 6 shows the deviations from the BCS formula for Pb No. 24 as computed from (9) using $l_{ph\,s}$ derived from the 51-MHz Pb No. 12 data. In this case the data showed a very slight frequency dependence as discussed in Sec. II B; also, (9) predicts a frequency dependence. The deviations from BCS given by (9) were calculated for each frequency investigated and the results were averaged to obtain the curve of Fig. 6.

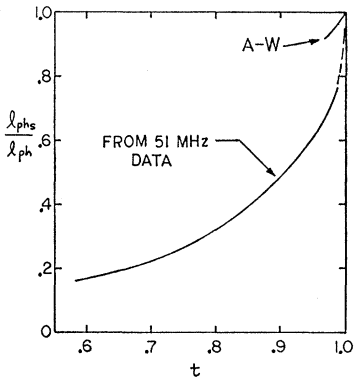

FIG. 8. Superconducting-to-normal ratio of the energy-averaged, phonon-limited mean free path as deduced from the 51-MHz Pb No. 12 data. The curve labeled "A-W" shows the phonon-limited free-path ratio for an electron energy of 0.6 meV calculated by Ambegaokar and Woo (Ref. 17).

The above analysis gives results in qualitative agreement with the main features exhibited by the experimentally determined attenuation ratio, but it fails on some important points. In pure lead at the lowest frequencies and near the transition, the experimentally determined R deviates less strongly from BCS than is predicted by (9), while (9) consistently underestimates the departures from BCS in the doped specimens. In pure lead (9) generally gives a weaker frequency dependence than is observed, but in the doped specimens (9) always gives a stronger frequency dependence than is found experimentally. There is a further inconsistency in that Pb No. 18 has a slightly smaller impurity-limited free path than Pb No. 24 (see Table I), so that on the basis of (9), one expects deviations from the BCS prediction to be more pronounced for Pb No. 24 than for Pb No. 18. However, the deviations from the BCS

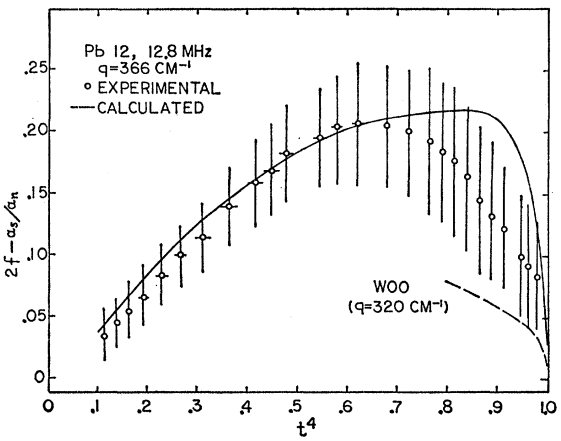

FIG. 9. Deviations from the BCS attenuation ratio for the Pb No. 12, 12.8-MHz data compared with those computed from Eq. (9). The calculation of Woo (Ref. 11) is also shown.

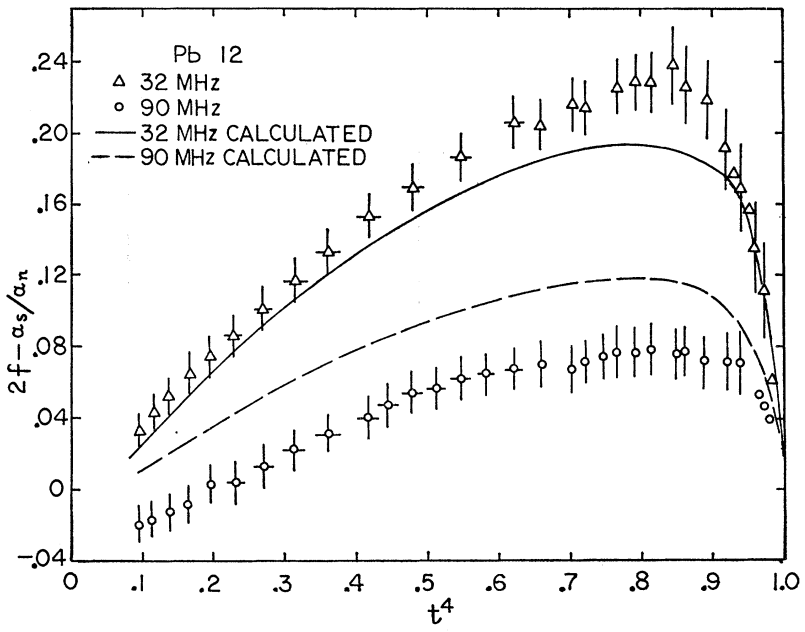

FIG. 10. Deviations from the BCS attenuation ratio for Pb No. 12 compared with those calculated from Eq. (9).

formula are slightly greater for Pb No. 18 than for Pb No. 24. Finally, it is to be observed that the mean-free-path analysis cannot even qualitatively explain the low-temperature behavior of the attenuation ratio shown in Fig. 4. At low temperatures, l is approximately impurity-limited, and for this case (9) reduces to the BCS result.

The goodness of fit to (9) is of course dependent on the assumed value of the zero-temperature energy gap. This choice is especially critical in the case of doped specimens, where the deviations from BCS are smaller than for pure lead and can partially be compensated by a slightly different choice of $\Delta(0)$. No effort was made to vary the value of the zero-temperature gap in order to obtain better agreement with (9) since such measures do not seem justified until the status of the theory is clarified.

III. CONCLUDING REMARKS

The electronic-attenuation ratio for lead almost always departs from the prediction of the BCS theory. The attenuation ratio is dependent on both impurity concentration and ultrasonic frequency and shows systematic behavior when these quantities are varied. Qualitatively different behavior is observed in the phonon-limited and impurity-limited regimes.

The difference in the frequency dependence of the electronic attenuation in the superconducting and normal states when the mean free path is phonon-limited, discussed in Sec. II D, gives experimental evidence in support of the idea that the phonon-limited free path is different in the normal and superconducting states. An analysis based on this idea, while not free from difficulties, shows that such a mean-free-path mechanism can qualitatively account for the main features exhibited by the attenuation ratio near the transition temperature. Thus, a mean-free-path change in the transition may be a major cause of the deviations of the data from the BCS prediction in the high-temperature range.

For reduced temperatures less than approximately 0.5 the data show deviations from the BCS formula that cannot be qualitatively explained by such a mean-free-path mechanism. In the low-temperature range the data for pure and doped specimens show the same qualitative behavior, and a strong-coupling calculation, valid in the impurity-limited case at low temperatures, would be of interest. For this case the energy dependence of the mean free path should be negligible, and departures from the BCS prediction presumably would be a consequence of the energy dependence or complex nature of the gap.

In concluding we briefly compare the results of the present measurements with results recently reported by others. Tittmann and Bömmel[5] have studied the ultrasonic attenuation in tin-doped lead. Near the transition temperature our data for tin-doped lead appear to be in essential agreement with theirs, but no quantitative comparison of the two sets of data was attempted since the impurity-limited free path for their specimens could not be determined sufficiently accurately from their published data. For reduced temperatures less than about 0.5 we find an attenuation ratio that decreases more slowly with decreasing temperature than the one reported by Tittmann and Bömmel.

Deaton[6] has investigated the attenuation of longitudinal ultrasound in [001]-oriented, high-purity, well-annealed lead. He finds that near the transition the

attenuation ratio falls most rapidly, indeed almost discontinuously, at the highest ultrasonic frequencies. This result directly contradicts our results on high-purity, deformed lead where the decrease in the attenuation ratio at the transition is observed to be less rapid at the highest frequencies than at the lower ones. If in fact Deaton's results are representative of amplitude-independent behavior for pure, well-annealed lead, one must conclude that some amplitude-independent dislocation mechanism is causing the discrepancy. The extent to which the normal-state data for the pure deformed and well-annealed doped specimens used for the present experiment correlate with each other and agree with the predictions of the free-electron model seems to rule out this mechanism for the specimens we studied.[1] Although it is hard to see how small amounts of cold work could modify the electronic attenuation of pure lead so greatly, the question can rigorously be settled only by obtaining amplitude-independent data in pure well-annealed lead to see if such a dislocation mechanism is operating in that case. To date, all our efforts to secure such data have failed, and we are aware of no published results for pure, well-annealed lead where explicit experimental proof of the amplitude independence of the results is given.

ACKNOWLEDGMENTS

We thank C. P. Newcomb and H. J. Willard for constructing some of the ultrasonic apparatus and for their many helpful discussions. Support from the National Science Foundation and the National Aeronautics and Space Administration is appreciated.

PHYSICAL REVIEW VOLUME 172, NUMBER 2 10 AUGUST 1968

Longitudinal Ultrasonic Attenuation in Pure Strong-Coupling Superconductors. II*

JAMES W. F. WOO

Department of Physics, Rutgers—The State University, New Brunswick, New Jersey

(Received 13 March 1968)

Previous work on low-frequency longitudinal ultrasonic attenuation in pure strong-coupling superconductors is extended to all values of ql (l=electron mean free path, q=phonon wave number). The result differs from that obtained for impurity scattering because vertex corrections are unimportant in the present problem. Numerical calculations of the reduced attenuation were performed for various values of q.

IN a previous paper[1] (to be referred to as I), expressions for the low-frequency longitudinal ultrasonic attenuation in pure strong-coupling superconductors in the $ql\gg1$ and $ql\ll1$ limits were derived (q=phonon wave number, l=phonon-limited electron mean free path) and numerical estimates of the reduced attenuation in lead for $ql<1$ were performed. In this paper, we extend the previous results to all values of ql and correct an error in the numerical work of I.

We first state some results obtained previously. We use the notation of I. Kadanoff and Falko[2] showed that the low-frequency longitudinal attenuation can be expressed as

$$\alpha(q,\omega)=\mathrm{Re}\frac{q^2}{i\omega\rho_{\mathrm{ion}}V_s}\{\langle[\tau_{zz},\tau_{zz}]\rangle(q,\omega)-(2p_F^2/3m)\times\langle[\tau_{zz},n]\rangle(q,\omega)+(p_F^2/3m)^2\langle[n,n]\rangle(q,\omega)\}. \quad (1)$$

We showed in I that

$$\lim_{\omega\to0}\mathrm{Re}(i\omega)^{-1}\left\langle\begin{Bmatrix}[\tau_{zz},\tau_{zz}]\\ [\tau_{zz},n]\\ [n,n]\end{Bmatrix}\right\rangle(q,\omega)=-\tfrac{1}{2}\int\frac{d\omega_1}{2\pi}\frac{\partial f(\omega_1)}{\partial\omega_1}\int\frac{d^3p}{(2\pi)^3}\begin{Bmatrix}p_z^4/m^2\\ p_z^2/m\\ 1\end{Bmatrix}\times\mathrm{tr}\tau_3\begin{Bmatrix}\tilde{f}_2\\ \tilde{f}_2{}^\tau\\ \tilde{f}_2{}^n\end{Bmatrix}(\epsilon_p,q,\omega_1). \quad (2)$$

* Supported in part by the National Science Foundation, the Office of Naval Research and the Rutgers Research Council.

[1] James W. F. Woo, Phys. Rev. **155**, 429 (1967).

[2] L. P. Kandanoff and I. I. Falko, Phys. Rev. **136**, A1170 (1964).